Journal of Molecular Structure 1198 (2019) 126910

Contents lists available at ScienceDirect

Journal of Molecular Structure

journal homepage: http://www.elsevier.com/locate/molstruc

Synthesis, anticancer evaluation *in vitro*, DFT, Hirshfeld surface analysis of some new 4-(1,3-benzothiazol-2-yl)-3-methyl-1-phenyl-4,5-dihydro-1*H*-pyrazol-5-one derivatives

Imane Chakib [a], Youness El Bakri [a, b, **], Chin-Hung Lai [c, d, *], Laila Benbacer [e], Abdelfettah Zerzouf [f], El Mokhtar Essassi [a], Joel T. Mague [g]

[a] Laboratoire de Chimie Organique Hétérocyclique, Centre de Recherche des Sciences des Médicaments, Pôle de Compétences Pharmacochimie, URAC 21, Faculté des Sciences, Université Mohammed V Rabat, Avenue Ibn Battouta, BP 1014, Rabat, Morocco
[b] Department of Organic Chemistry, Faculty of Science, RUDN University Miklukho-Maklaya St. 6, 117198, Moscow, Russian Federation
[c] Department of Medical Applied Chemistry, Chung Shan Medical University, Taichung, 40241, Taiwan
[d] Department of Medical Education, Chung Shan Medical University Hospital, 402, Taichung, Taiwan
[e] Unité de Biologie et Recherche Médicale, Centre National de l'Energie, des Sciences et des Techniques Nucléaires, (CNESTEN), BP 1382 RP, 10001, Rabat, Morocco
[f] Laboratoire de Chimie Organique et Etudes Physicochimique, ENS Takaddoum, Rabat, Morocco
[g] Department of Chemistry, Tulane University, New Orleans, LA, 70118, USA

ARTICLE INFO

Article history:
Received 13 March 2019
Received in revised form
4 August 2019
Accepted 7 August 2019
Available online 10 August 2019

Keywords:
1,3-Benzothiazole
Pyrazole
Alkylation
Anticancer
Crystal structure
DFT

ABSTRACT

A new method for synthesizing compounds having benzothiazole and pyrazole moieties in their backbone has been successfully performed, based on the rearrangement of pyrazolylylidene-pyranopyrazolone in the presence of o-aminothiophenol in hot *n*-butanol. The new compound has been alkylated with different alkylating agents under phase transfer catalysis conditions. A Hirshfeld surface analysis for visually analyzing intermolecular interactions in crystal structures employing molecular surface contours and 2D fingerprint plots has been used to examine molecular shapes. The gas-phase geometries of the new compound and one alkylated derivative were studied by the DFT-B3LYP method. The anticancer properties of the compounds obtained have been evaluated.

1. Introduction

Heterocyclic compounds are ubiquitous in nature [1] and the synthesis of functionalized heterocyclic molecules has remained an attractive target because of their many applications in the pharmaceutical industry [2,3]. Functionalized 1,4-benzothiazines containing benzene fused with a six-membered thiazine ring represent an important class of heterocyclic compounds which exhibit many biological properties such as antimicrobial [4,5], antifungal [4], 15-lipoxygenase inhibitor [4], *anti*-HIV [4], neuroleptics [4], antirheumatic [4], calcium antagonist [4] antioxidant [4], cardiovascular [4], antimalarial [4], and anthelmintic activities [4]. Apart from versatile pharmaceutical applications, the 1,4-benzothiazine is a subunit of many natural pigments, dyestuffs and is also present in one type of melanin, pheomelanin [6,7].

Because of the versatile applications of this heterocyclic scaffold, a plethora of synthetic methods has been developed. The most straightforward approach for its synthesis is the direct condensation-cyclization between 2-aminobenzenethiol and a 1,3-dicarbonyl compound in the presence of various reagents/catalysts. Some notable examples are the use of DMSO [8–10], H_2O_2 [11], Baker's yeast [12] and hydrazine hydrate [13]. Most of these routes suffer from one or more constraints such as the use of strongly basic

* Corresponding author. Department of Medical Applied Chemistry, Chung Shan Medical University, Taichung, 40241, Taiwan.
** Corresponding author. Laboratoire de Chimie Organique Hétérocyclique, Centre de Recherche des Sciences des Médicaments, Pôle de Compétences Pharmacochimie, URAC 21, Faculté des Sciences, Université Mohammed V Rabat, Avenue Ibn Battouta, BP 1014, Rabat, Morocco.
E-mail addresses: yns.elbakri@gmail.com (Y. El Bakri), chlai125@csmu.edu.tw (C.-H. Lai).

https://doi.org/10.1016/j.molstruc.2019.126910
0022-2860/

media, strong oxidizing agents, high temperature as well as the formation of disulfide by-product [13,14] or decomposition of the intermediate to benzothiazole [15]. In another synthetic approach, the microwave-assisted synthesis of 1,4-benzothiazine has been reported [16].

In a continuation of our previous work on the synthesis of new heterocyclic derivatives [17–21], we are interested in the synthesis of heterocyclic systems containing both benzothiazole and pyrazole moieties and the evaluation of their biological activities.

We have shown that dehydroacetic acid constitutes an interesting precursor in the synthesis of several heterocyclic compounds. Thus 5-methyl-4-(3,4-dimethyl-1-phenyl-3a,7a-dihydropyrano[2.3-c]pyrazol-6(1*H*)-ylidene)-2-phenyl-2.4-dihydro-3*H*-pyrazol-3-one was prepared by the action of phenylhydrazine in refluxing acetic acid [22]. It is worthy to note that the literature reports little work concerning the reactivity of this molecule with respect to nucleophilic reagents [23].

In this work we report the condensation of 5-methyl-4-(3,4-dimethyl-1-phenyl-3a,7a-dihydropyrano[2.3-*c*]pyrazol-6(1*H*)-ylidene)-2-phenyl-2.4-dihydro-3*H*-pyrazol-3-one with 2-aminothiophenol in refluxing *n*-butanol. We have been able to isolate a new heterocyclic system containing benzothiazole and pyrazole moieties, namely 4-(1,3-benzothiazole-2-yl)-3-methyl-1-phenyl-2-pyrazolin-5-one as well as a bipyrazolic compound. Alkylation of the former compound generated a series of new heterocyclic compounds which have been studied to assess their antitumor and antibacterial activities.

2. Methods and materials

2.1. Chemistry

The melting points were measured with Köfler bench or Büchi Melting Point B-545 instruments. The nuclear magnetic resonance spectra (^{1}H, ^{13}C, DEPT) were recorded on a Brüker AVANCE 300 instrument operating at 300 MHz. The chemical shifts are given in ppm (parts per million) with respect to the TMS internal reference. The coupling constants (J) are expressed in hertz (Hz) and the multiplicity is represented as follows: singlet (s), doublet (d), doublet doubled (dd), triplet (t), multiplet (m) and quadruplet (q). Mass spectra were performed on a PerkinElmer SCIEX API unit 300. The samples are ionized by the electrospray technique (ESI). Elemental analysis was performed on a Euro EA-CHNSO Elemental Analyzer. The evolution of the reactions is followed by thin layer chromatography on aluminum sheets coated with Merck 60 F254 silica gel (0.2 nm thick). The imaging of the plates is carried out under an ultraviolet lamp at 254 nm. The purifications by column chromatography are carried out on Merck silica gel 40–70 μm (230–400 mesh). X-ray crystal structure data were collected on a Bruker Smart APEX CCD diffractometer with graphite monochromated Mo K_α radiation of wavelength $\lambda = 0.71073$ Å.

2.2. The action of 2-aminothiophenol 2 on the compound (1)

2-aminothiophenol (0.014 mol) and 5-[1-phenyl-3-methyl-5-oxo-pyrazol-4-ylidene]-1,7-dimethyl-3-phenylpyrano[2,3-*c*]pyrazole (0.0025 mol) was refluxed in 50 mL of *n*-butanol for 72 h. The product, 4-(1,3-benzothiazole-2-yl)-3-methyl-1-phenyl-2-pyrazolin-5-one **3**, precipitates first in 50% yield. After filtration and concentration of the solution under reduced pressure the second product bipyrazole (**4**) was isolated in low yield (Scheme 1).

Yield: 50%; m.p: 187; M = 307.36 g/mol; ^{1}H NMR (DMSO-d_6, 300 MHz) δ, 9.7 (s, 1H, H-N), 2.4 (S, 3H, CH_3), 7.16–8.02 (m, 9H, $H_{aromatic}$). ^{13}C NMR (DMSO-d_6, 75 MHz) δ, 14.81, 161.79, 146.11, 140.71, 138.74, 126, 115.26, 96, 43, 128, 99, 128.82, 127.83, 124.84, 124.57, 122.09, 119.47, 115.26.

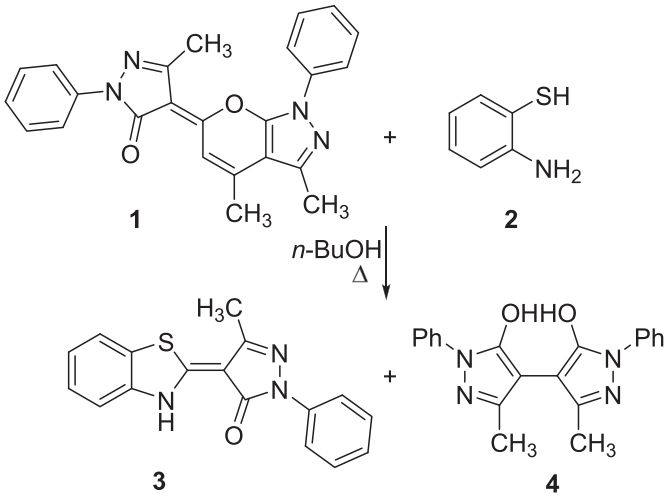

Scheme 1. The structure of compound **3** was elucidated from spectral data (^{1}H and ^{13}C NMR) as well as by single crystal X-ray diffraction.

The ^{1}H NMR spectrum of **3**, in $CDCl_3$ shows signals corresponding to the aromatic protons, a signal at 2.4 ppm due to the protons of the pyrazolic methyl group and a signal at 9.7 ppm assigned to the NH group of the benzothiazole ring.

The ^{13}C NMR spectrum of **3** shows signals assigned to the quaternary carbons, the carbons of the aromatic rings, a signal at 161.79 ppm corresponding to the carbonyl group and a signal at 14.81 ppm attributable to the pyrazolic methyl group.

2.2.1. Synthesis of 3,3′-dimethyl-1,1′-diphenyl-1H,1′H-[4,4′-bipyrazole]-5,5′-diol (4)

Yield: 15%; m.p: 115–117; ^{1}H NMR (DMSO-d_6, 300 MHz) δ, 3.40 (s, 1H, C-CH_3), 7.33–8,12 (m, 9H, H_{ar}), 11.83 (s, 1H, OH). ^{13}C NMR (DMSO-d_6, 75 MHz) δ: 13.08, 112.29, 121.35, 129.3, 129.54, 133.48, 133.94, 151.16, 152.33. HRMS (ESI) Calculated for $C_{18}H_{15}N_3OS$: $[M + H^+] = 346.1420$, Found: $[M + H^+] = 346.1422$. Elemental analysis Calculated: C, 69.35%; H, 5.24%; N, 16.17%; O, 9.24%, Found: C, 69.35%; H, 5.23%; N, 16.16%; O, 9.26%.

2.3. X-ray data collection, structure solution and refinement

The structures of compounds **3** and **6′** have been confirmed by single-crystal X-ray crystallographic studies. A suitable crystal of **3** was mounted on a polymer loop and placed in the cold nitrogen stream on the diffractometer. A full sphere of data was collected under control of the APEX3 software [24] and reduced to F^2 values with SAINT [24] which also performed a global refinement of the unit cell parameters. An empirical absorption correction and merging of equivalent reflections were carried out with SADABS [24], the structure was solved by direct methods (SHELXT [25]) and refined by full-matrix, least-squares procedures (SHELXL [26]). The H-atoms were located in a difference map and refined with isotropic displacement parameters. The structure of **6'** was performed similarly except at room temperature which necessitated affixing the crystal to a nylon loop with a drop of epoxy cement. While all H-atoms could be located in a final difference map, the greater extent of vibrational motion made including them as riding contributions in idealized positions with isotropic displacement parameters tied to those of the attached atoms a more reasonable model.

2.4. Alkylation of compound (3)

(0.01 mol) of compound **3** and potassium carbonate K_2CO_3 (0.01 mol) were dissolved in 50 mL of *N*,*N*-dimethylformamide (DMF) and the desired alkyl halide (0.02 mol) and tetra-*n*-butylammonium bromide as a catalyst (0.001 mol) were added to the solution which was stirred at room temperature for 24 h. The residue obtained after evaporation of the solvent was recrystallized from dichloromethane/hexane to afford the major product and the second product was obtained from the filtrate by column chromatography on silica gel (eluent: ethyl acetate/hexane (1/9).

2.4.1. The action of methyl iodide

2.4.1.1. 4-(1.3-benzothiazol-2-yl)-2,3-dimethyl-1-phenyl-3-pyrazolin-5-one (5). Yield: 80%; m.p: 214–216; ^{1}H NMR (DMSO-d_6, 300 MHz) δ, 3 (s, 1H, C-CH_3), 3,36 (s, 3H, N-CH_3), 7,27–8,09 (m, 9H, H_{ar}). ^{13}C NMR (DMSO-d_6, 75 MHz) δ, 13.08, 34.5, 163.29, 121.35, 129.54, 102.08, 133.483, 133.89, 151.12, 152.29, 160.67. HRMS (ESI) Calculated for $C_{18}H_{15}N_3OS$: $[M + H^+]$ = 321.0911, Found: $[M + H^+]$ = 321.0913. Elemental analysis Calculated: C, 67.27%; H, 4.70%; N, 13.07%; O, 4.98%, S, 9.98% Found: C, 67.28%; H, 4.69%; N, 13.08%; O, 4.97%, S, 9.98%.

2.4.2. The action of allyl bromide

2.4.2.1. 4-(1.3-benzothiazol-2-yl)-3-methyl-1-phenyl-2-(prop-2-enyl)-3-pyrazolin-5-one (6). Yield: 80%; m.p: 144–146; ^{1}H NMR (DMSO-d_6, 300 MHz) δ: 7.42–8.03 (m, 9H, $H_{aromatic}$), 2.9 (s, 1H, CH_3), 4,3 (d, 2H, J = 5.7 Hz, N-CH_2), 5.6 (m, 1H, CH=), 5.2 (dd, 2H, J_{trans} = 17 Hz, J_{cis} = 10 Hz, C=CH_2). ^{13}C NMR (DMSO-d_6, 75 MHz) δ: 12.8, 49.05, 119.71, 163.77, 121.52, 121.68, 124.06, 125.75, 125.85, 128.16, 129.46, 129.80, 160.32, 152.60, 152.22, 134.02, 133.98, 103.73. HRMS (ESI) Calculated for $C_{20}H_{17}N_3OS$: $[M + H^+]$ = 347.1102, Found: $[M + H^+]$ = 347.1105. Elemental analysis Calculated: C, 69.14%; H, 4.93%; N, 12.09%; O, 4.60%, S, 9.23% Found: C, 69.15%; H, 4.94%; N, 12.06%; O, 4.61%, S, 9.24%.

2.4.3. The action of propargyl bromide

2.4.3.1. 4-(1.3-benzothiazol-2-yl)-3-methyl-1-phenyl-2-(prop-2-ynyl)-3-pyrazolin-5-one (7). Yield: 85%; m.p: 169–171, ^{1}H NMR (DMSO-d_6, 300 MHz) δ, 2.946 (s, 1H, C-CH_3), 4.625 (s, 2H, CH_2), 3.399 (s, 1H, C-H), 7.365–8.091 (m, 9H, $H_{aromatic}$); ^{13}C NMR (DMSO-d_6, 75 MHz) δ, 12.98, 37.85, 163.59, 122.16, 129.94, 159.617, 155.514, 152.647, 134.266, 133.801, 104.937. HRMS (ESI) Calculated for $C_{20}H_{15}N_3OS$: $[M + H^+]$ = 345.0923, Found: $[M + H^+]$ = 345.0925. Elemental analysis Calculated: C, 69.54%; H, 4.38%; N, 12.17%; O, 4.63%, S, 9.28% Found: C, 69.55%; H, 4.36%; N, 12.18%; O, 4.64%, S, 9.27%.

2.5. Computational method

2.5.1. DFT calculation

The structures in the gas phase of **3** and **6′** were optimized by means of density functional theory. The DFT calculation was performed by the hybrid B3LYP method, which is based on the idea of Becke and considers a mixture of the exact (HF) and DFT exchange utilizing the B3 functional, together with the LYP correlation functional [27,28]. In conjunction with a double-ξ basis set, ADZP, the B3LYP calculations were done [29]. After obtaining the converged geometry, the harmonic vibrational frequencies were calculated on the same theoretical level to confirm that the number of imaginary frequencies is zero for the stationary point. Both the geometry optimizations and harmonic vibrational frequency analyses of **3** and **6'** were done by the Gaussian 16 program [30].

2.5.2. The Hirshfeld surface calculations

Both the definition of a molecule in a condensed phase and the recognition of distinct entities in molecular liquids and crystals are fundamental concepts in chemistry. Based on Hirshfeld's partitioning scheme, Spackman et al. in 1997 proposed a method to divide the electron distribution in a crystalline phase into molecular fragments [31–33]. Their method partitioned the crystal into regions where the electron distribution of a sum of spherical atoms for the molecule dominates over the corresponding sum of the crystal. Because it was derived from Hirshfeld's stockholder partitioning, the molecular surface is named as the Hirshfeld surface. In this study, the Hirshfeld surface analysis of **3** and **6′** was performed utilizing the CrystalExplorer program [34].

2.6. Anticancer activity screening

The new derivatives (**3**, **5**, **6** and **7**) are solubilized in dimethyl sulfoxide (DMSO) before being incorporated into the culture medium. The final concentration of DMSO in the different solutions is less than 0.01%. A series of dilutions of the new compounds is carried out with the culture medium in order to evaluate different concentrations. For the evaluation of our products, we chose a concentration range from 50 to 1.56 μg/mL.

Cells are seeded in 96 well plates at the appropriate density for each line and cultured for 24 h at 37 °C. After incubation, the products to be tested are deposited at different concentrations in duplicate in the wells. The plates are then incubated for 48 h at 37 °C. Four hours before the end of the incubation, 10 μL of an MTT solution (5 mg/mL) is added to the wells. The plates are incubated for 4 h at 37 °C in the presence of 5% CO_2. Formation of the blue crystals of formazan is visualized under an optical microscope. The culture medium is removed and the same volume of DMSO (Sigma) is added to each well. The plate is then subjected to gentle agitation allowing the dissolution of the formazan crystals. The absorbance is determined at 570 nm in a microplate reader and the results are expressed as percent viability of the treated versus untreated cells. Untreated cells are considered a control with a percentage of viability of 100%. The cytotoxicity index is calculated using the following formula:

$$\%IC = (1 - (T/C))\text{x}100$$

T and C: average optical densities of the tested fractions and controls.

Mitomycin C was used as a positive control of our experiment. Mitomycin C is an antineoplastic and antibiotic substance extracted from Streptomyces caespitosus. It has an alkylating effect:

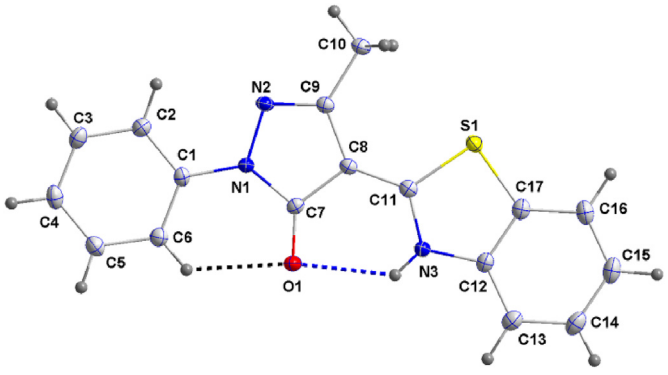

Fig. 1. Perspective view of 3 with labeling scheme and 50% probability ellipsoids. Intramolecular hydrogen bonds are shown by dashed lines.

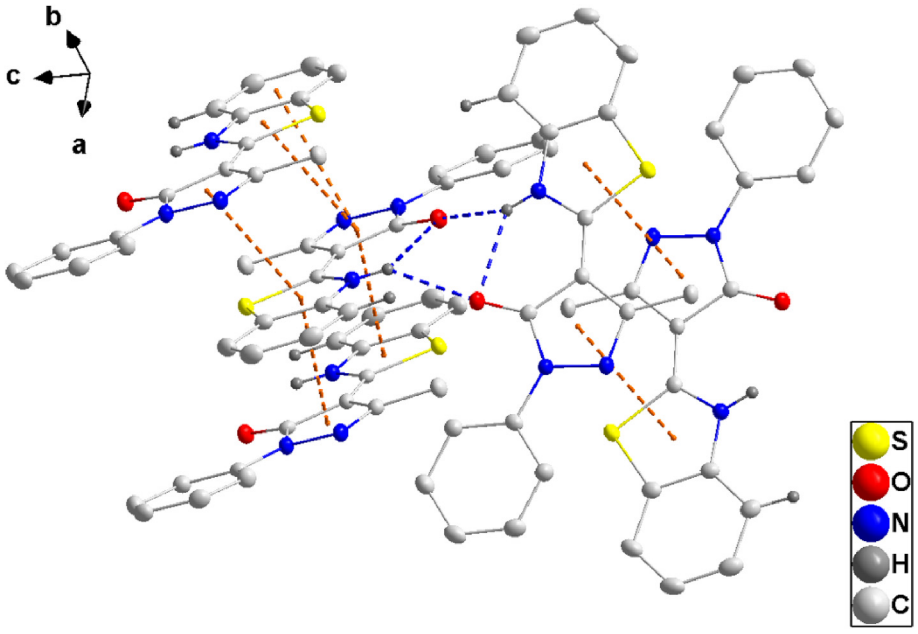

Fig. 2. Detail of the bifurcated N–H···O hydrogen bonds (blue dashed lines) and the π-stacking interactions (orange dashed lines).

Table 1
Hydrogen-bond geometry of 3.

D—H···A	D—H	H···A	D···A	D—H···A
N3—H3A···O1	0.822(17)	2.258(18)	2.8500(13)	129.3(15)
N3—H3A···O1^{i}	0.822(17)	2.261 (17)	2.9198(14)	137.5(16)
C6—H6···O1	0.931(16)	2.317(15)	2.9627(15)	126.2(12)
C13—H13···O1^{i}	0.993(15)	2.621(14)	3.2432(16)	120.8(10)

Symmetry code: (i) −x+1, y, −z+1/2.

formation of adducts with the DNA, action particularly marked in phases G1 and S.

2.6.1. Cell maintenance and culture conditions

The cell line chosen for our cytotoxicity assays is the HEp-2 line (ATCC No. CCL-23). These are epithelial type cells which are adherent and derived from the culture of tumor cells of human origin (laryngeal carcinoma). The cells are cultured in a suitable medium DMEM (essential minimum Eagle medium) supplemented with 10% fetal calf serum (FCS) and a mixture of Penicillin/Streptomycin antibiotics. The cell lines are maintained at 37 °C in an atmosphere saturated with moisture and containing 5% of CO_2.

The cells are grown in monolayers and after three days are observed under a reversed phase contrast microscope. When the cells reach a subconfluent growth state, the culture medium is

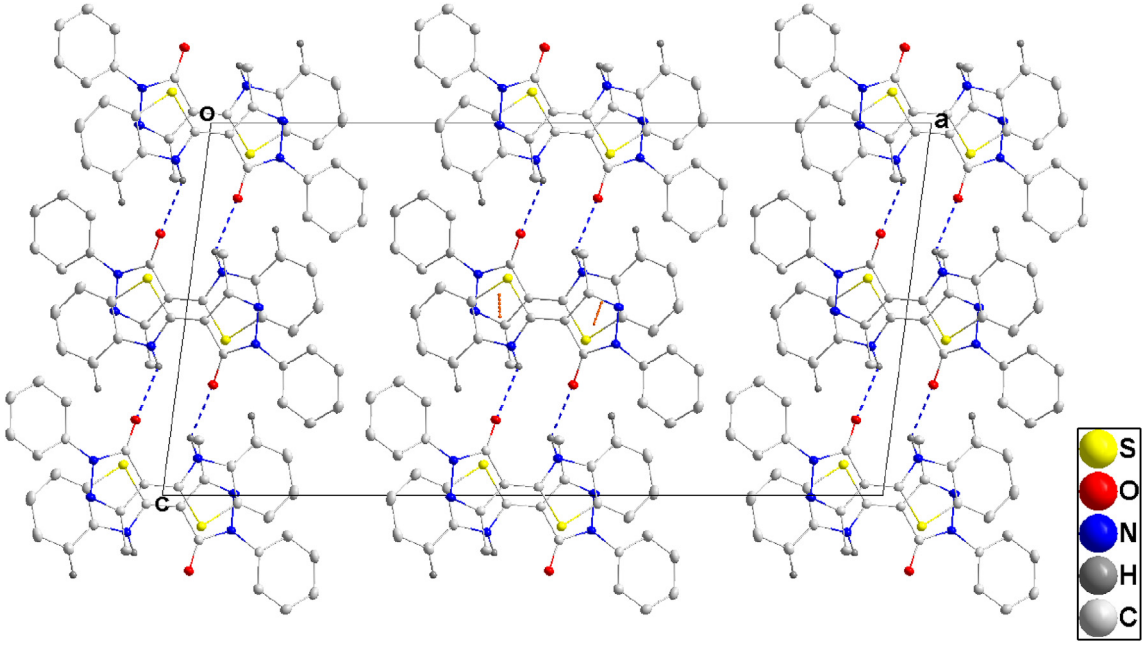

Fig. 3. Packing viewed along the *b*-axis direction with a portion of the π-stacking shown by orange dashed lines and the N–H···O hydrogen bonds connecting the stacks by blue dashed lines.

aspirated and the cells are washed with PBS (phosphate buffered saline).

The cells are then detached with 500 µL of trypsin/EDTA (ethylenediaminetetraacetic acid) for 5 min at 37 °C and taken up in 10 mL of new culture medium. The cells are then enumerated using a Malassezhematimeter. Their viability is assessed by the trypan blue exclusion method.

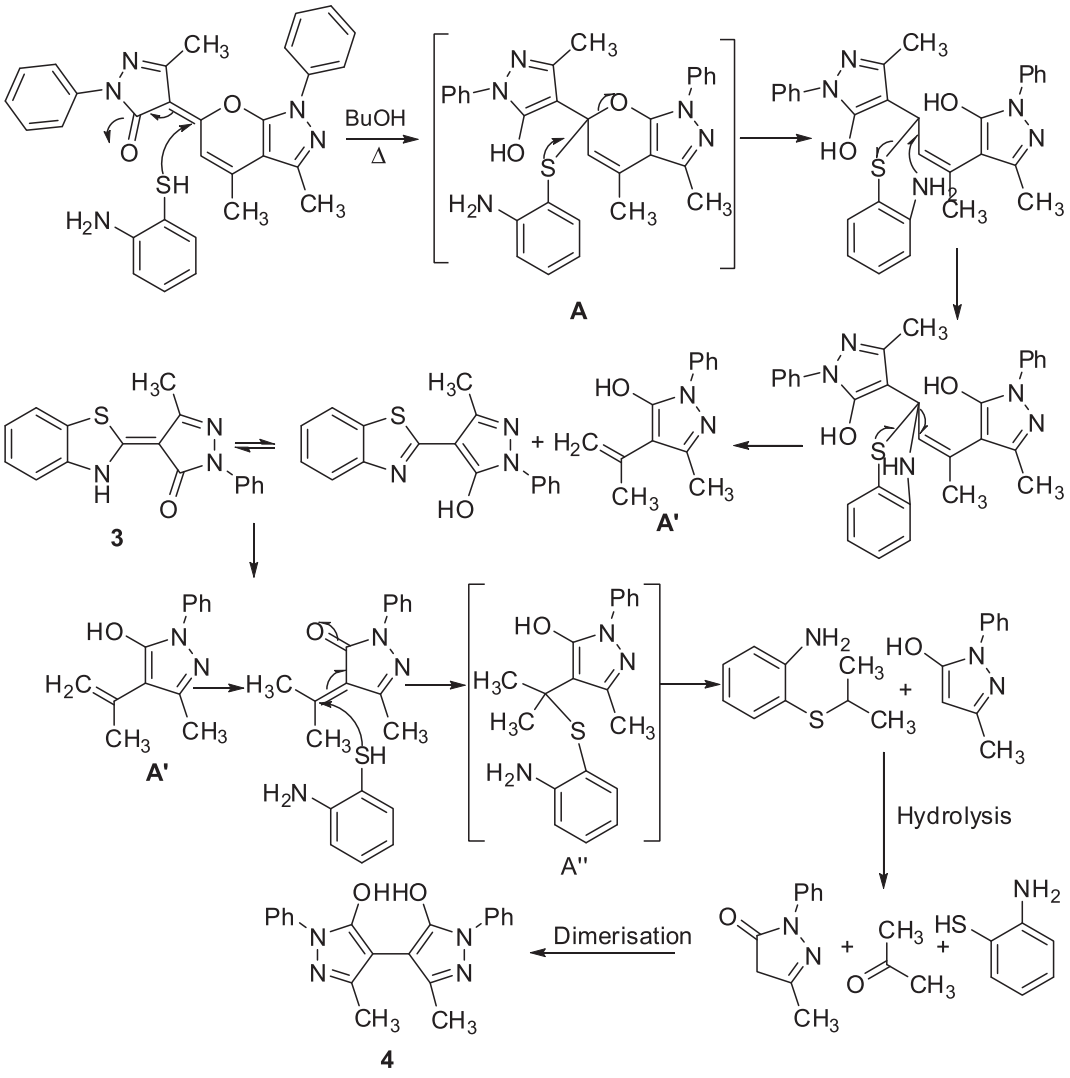

Scheme 2. A plausible mechanism of the formation of the compounds 3 and 4.

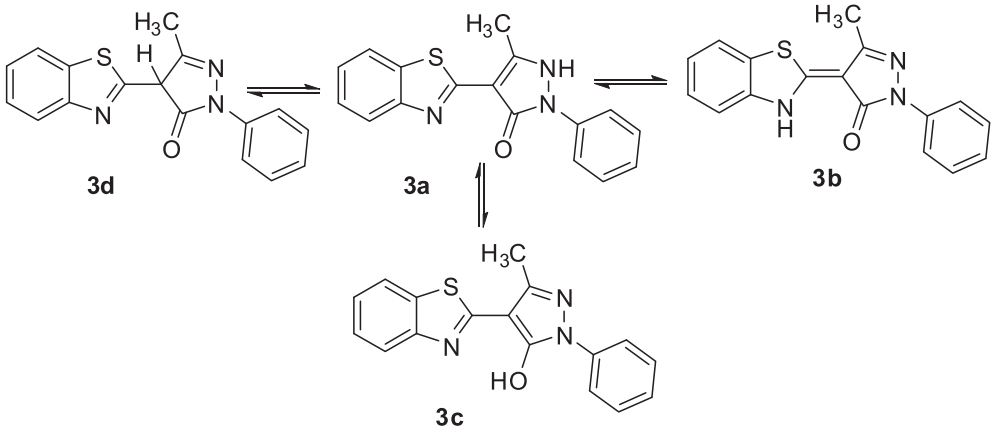

Scheme 3. Tautomeric forms of compound 3.

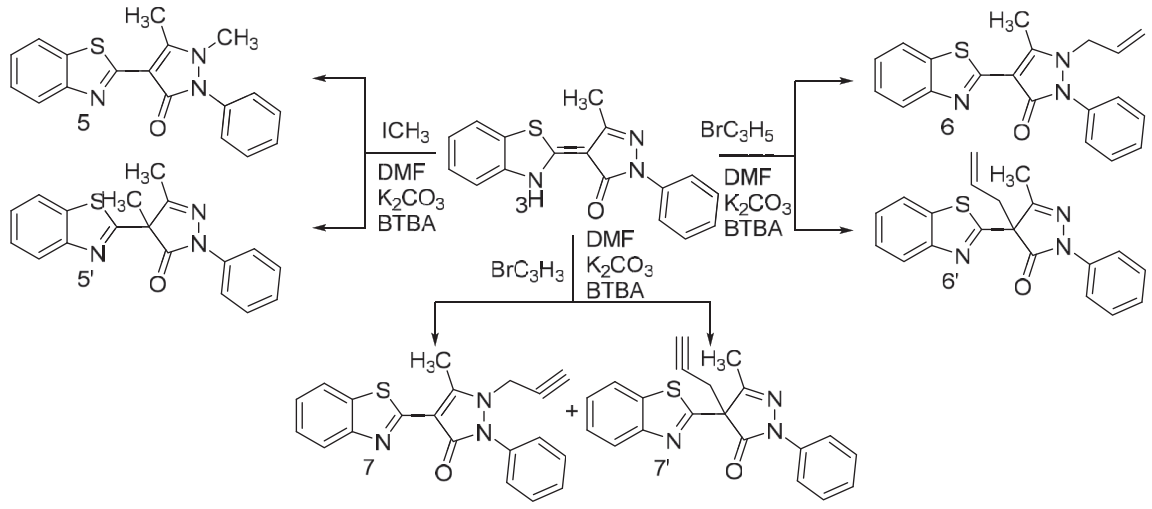

Scheme 4. It is significant that in no case was it possible for us to isolate a compound resulting from alkylation of the nitrogen atom of the benzothiazole moiety or of the oxygen atom of the hydroxyl group. Also, compounds **5**–**7** possess a structure similar to that of the antipyrine, especially compound **5.**

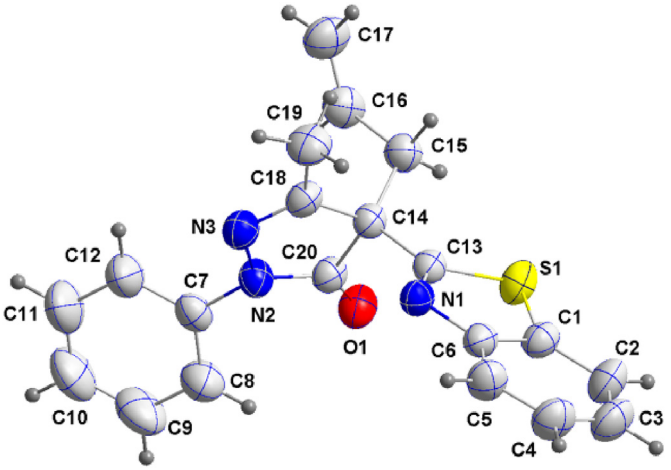

Fig. 4. Diagram with the labeling scheme and 50% probability ellipsoids for 6′.

Table 2
Hydrogen-bond geometry of compound 6'

D—H···A	D···A
C3—H3···O1^{i}	3.4589 (19)
C15—H15A···O1^{ii}	3.4759 (16)
C17—H17B···Cg3^{iii}	3.6098 (18)

Symmetry codes: (i) −x+3/2, y−1/2, −z+3/2; (ii) −x+1/2, y−1/2, −z+3/2; (iii) −x+1/2, y+1/2, −z+3/2.

2.6.2. Evaluation of cell viability

To estimate cell viability, we performed a trypan blue exclusion test. This test is based on the ability for live cells to exclude high molecular weight dyes. Trypan blue (0.4% PBS) (Sigma-Aldrich) is added to the cell suspension. Counting is performed on counting slides: Mallassez's blade. Trypan blue is actively excluded from living cells but it enters the cytoplasm of dead cells. In light microscopy, the dead cells are stained blue while the living cells remain colorless [35].

3. Results and discussion

3.1. Description of the crystal structure of compound 3

The molecule of **3** is slightly bowed along its length as indicated by the dihedral angles of 7.46(7)° and 6.20(5)° between the central 5-membered ring and, respectively, the phenyl ring and the benzothiazole unit. The near planarity of the molecule is largely the result of the intramolecular N3—H3A···O1 and C6—H6···O1 hydrogen bonds (Fig. 1). The bond distances are generally consistent with the Lewis structure shown for tautomer **3b** (Scheme 3), particularly the C9—N2 distance of 1.3111(16) Å. Interestingly, the C11—N3 distance of 1.3483(16) Å is shorter than the C8—C11 distance of 1.3920(17) Å which is unexpected and we have no ready explanation for this.

Head-to-tail π-stacking interactions between pyrazole and benzothiazole rings generate stacks along the *b*-axis direction (Fig. 2). In these, the centroid … centroid distance between the C7···C9/N2/N1 and C12/C17/S1/C11/N3 rings alternates between 3.8519(8) and 3.7285(8) Å along the stack. The stacks are tied together by C13—H13···O1 and bifurcated N3—H3A···O1 hydrogen bonds (Table 1 and Figs. 2 and 3).

3.2. Mechanism of the formation of compounds 3 and 4

A plausible mechanism for the formation of **3** from the condensation of 2-aminothiophenol with 5-methyl-4-(3,4-dimethyl-1-phenyl-3a,7a-dihydropyrano[2,3-*c*]pyrazol-6(1*H*)-ylidene)-2-phényl-2.4-dihydro-3*H*-pyrazol-3-one **1**, is as follows:

The nucleophilic attack of the amino group of 2-aminothiophenol **2** on the carbon at the 9-position of the pyranic ring in **1** leads to the ring opening of the pyranic moiety giving the intermediate [A] (Scheme 2). Subsequently, the formation of the benzothiazole ring occurs by nucleophilic attack of the SH group of the intermediate [A'] on the iminic carbon leading to an intramolecular cyclization rearrangement and loss of a pyrazolic derivative (A″). In addition, the 2-aminothiophenol, being in excess in the reaction medium, makes a second attack on the intermediate [A"] leading to [A"'] and pyrazolone which, after dimerization, leads

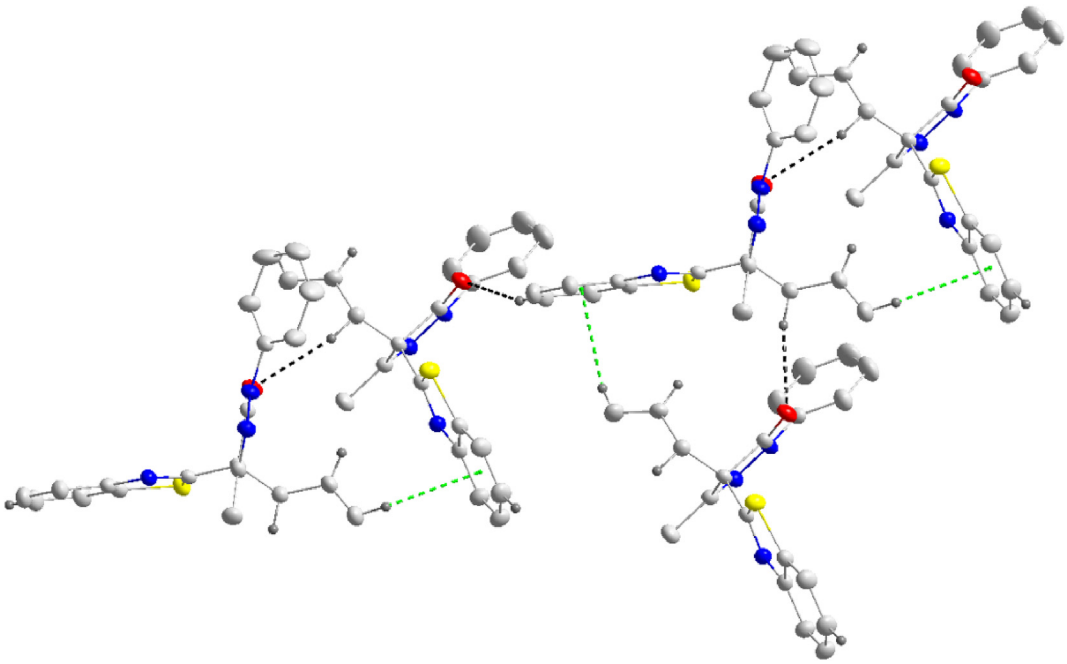

Fig. 5. Detail of one chain in 6′ formed by C—H···O hydrogen bonds (black dashed lines) and C—H···π(ring) interactions (green dashed lines).

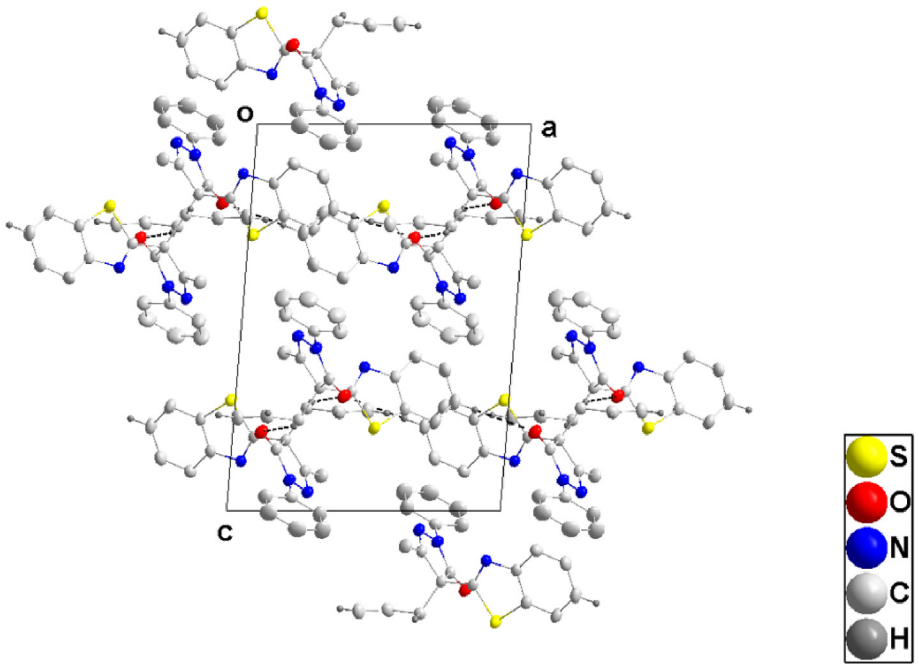

Fig. 6. Packing in 6′ seen along the *b*-axis direction providing edge views of two layers with the C—H···O hydrogen bonds shown as dashed lines.

to the formation of bipyrazole **4**.

3.3. Alkylation of 4-(1,3-benzothiazole-2-yl)- 3-methyl-1-phenyl-2-pyrazolin-5-one 3

Having efficiently obtained compound **3**, and for the purpose of preparing a series of monosubstituted derivatives of 4-(1,3-benzothiazole-2-yl)-3-methyl-1-phenyl-2-pyrazolin-5-one **3** we used solid-liquid phase transfer catalysis conditions.

In the liquid state, **3** can exist in the tautomeric forms **3a**, **3b**, **3c**, and **3d** while **3b** is the most stable in the solid state (Scheme 3).

We carried out the alkylation reaction of 4-(1,3-benzothiazole-2-yl)-3-methyl-1-phenyl-2-pyrazolin-5-one **3** by different alkylating agents in *N*,*N*-dimethylformamide in the presence of potassium carbonate as a base and tetra-*n*-butylammonium bromide (TBAB) as the catalyst.

In all cases, we were able to isolate two compounds. The major compound corresponding to the *N*-alkylation precipitates from the

Table 3
Crystal data and parameters for structure refinement of 3 and 6'

Compound	3	6′
CCDC deposit No	CCDC 1894222	CCDC 1894223
Chemical formula	$C_{17}H_{13}N_3OS$	$C_{20}H_{17}N_3OS$
Formula weight	307.36	347.42
Temperature (K)	100(2)	296(2)
Crystal size (mm)	0.188 × 0.219 x 0.244	0.41 × 0.37 × 0.26
Crystal system	monoclinic	monoclinic
Space group	C 2/c	$P2_1/n$
a, b, c (Å)	27.029(3),7.4019(7), 14.0657(14)	11.0064(4), 10.6756(4), 15.5992(7)
β (°)	97.475 (1)	94.626 (1)
Volume(Å^3)	2790.2 (5)	1826.93 (13)
Z	8	4
Radiation type	Mo Kα	Mo Kα
μ (mm^{-1})	0.24	0.19
Data collection		
Diffractometer	Bruker Smart APEX CCD	Bruker Smart APEX CCD
Absorption correction	Multi-scan SADABS (Bruker, 2016)	Multi-scan SADABS (Bruker, 2016)
No. of measured, independent and observed [I > 2σ(I)] reflections	26030, 3717, 3122	15765, 4901, 3093
R_{int}	0.034	0.070
$(\sin\theta/\lambda)_{max}$ (Å^{-1})	0.684	0.684
Refinement		
No. of reflections	3717	4901
No. of parameters	251	227
H-atom treatment	All H-atom parameters	Riding
$\Delta\rho_{max}$, $\Delta\rho_{min}$ (e Å^{-3})	0.82, −0.23	0.24, −0.25

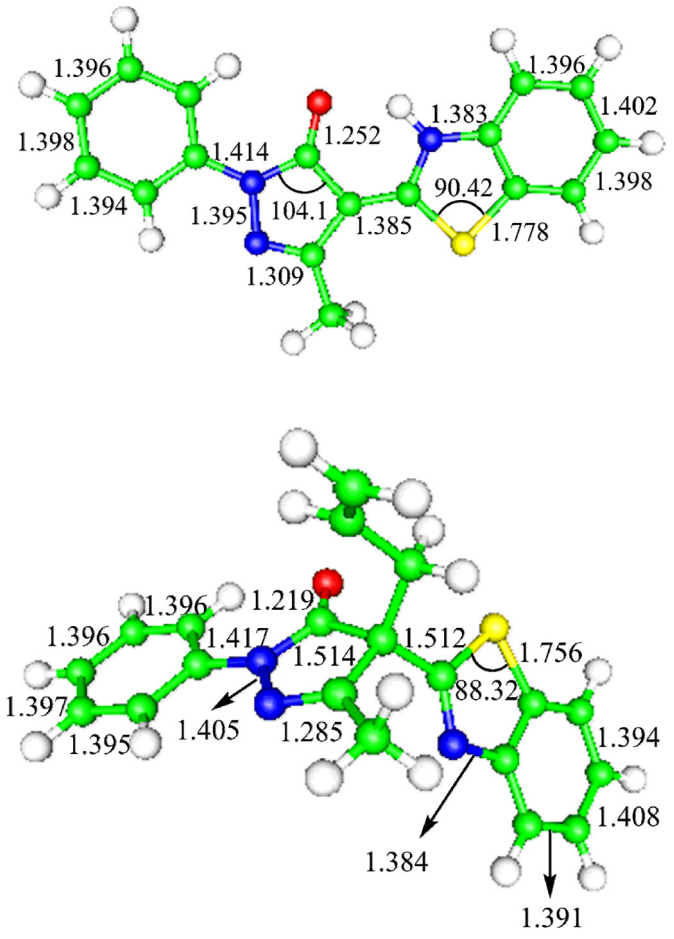

Fig. 7. The B3LYP-optimized geometries of 3 and 6'.

reaction mixture and was obtained in about 80% yield (Scheme 4).

The structures of the new compounds were confirmed by NMR (^{1}H and ^{13}C) spectral data and single crystal X-ray diffraction. For example, the diagram of **6'** is depicted in Fig. 4.

3.4. Description of the crystal structure of compound 6'

The benzothiazine moiety is planar to within 0.038(1) Å with an r.m.s. deviation of the fitted atoms of 0.001. Its mean plane is inclined to that of the N2/N3/C18/C14/C20 ring by 74.96(6)° while the angle between the mean planes of the N2/N3/C18/C14/C20 and C7···C12 rings is 35.72(8)°. The bond distances are generally in accord with the Lewis structure for **6'** shown in Scheme 4. Thus the C13—N1 and C18—N3 distances are, respectively, 1.2802(17) and 1.2864(17) Å while the C13—C14 distance is 1.5094(17) Å. In the crystal, alternating C3—H3···O1 and C15—H15A···O1 hydrogen bonds, together with C17—H17B···*Cg*3 interactions (Table 2; *Cg3* is the centroid of the C1•••C6 ring) form chains parallel to (110) (Fig. 5). These chains are associated through C3—H3···O1 and C15—H15A···O1 hydrogen bonds to form layers parallel to [001] which have the phenyl groups on the outside surfaces (Fig. 6). Furthermore, the data and parameters for structure refinement of **3** and **6'** are summarized in Table 3.

3.5. The DFT results of 3 and 6'

The DFT-B3LYP functional was used to optimize the gas-phase geometries of compounds **3** and **6′** with the results shown in Fig. 7. In contrast with **3**, **6′** has an additional -CH_2-CH=CH_2 group. As depicted in Fig. 7, it is found that the optimized geometry of **3** shows a discrepancy from that of **6'**.

3.6. The Hirshfeld surface analyses of 3 and 6'

The standard resolution molecular Hirshfeld surface (d_{norm}) of **3** and **6'**are shown in Fig. S1. The surface is shown as transparent so the molecular moiety can be visualized in a similar orientation for all of the structures around which they were calculated. The 3D d_{norm} surface could be used to identify very close intermolecular interactions. The value of d_{norm} is negative (positive) when

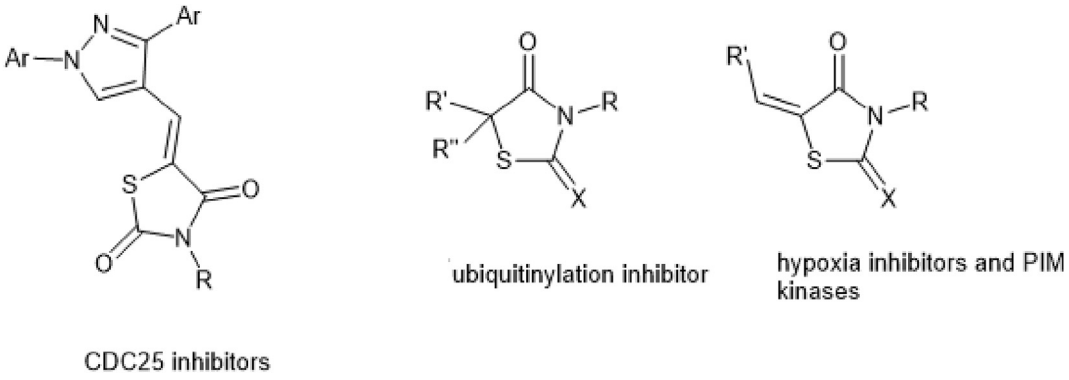

Scheme 5. The objective of this study is to test new heterocyclic systems that bring together two large classes of compounds known for their antitumor activity (pyrazole and benzothiazole). Thus we tested the anti-tumor activity of compound 3 and its alkylated derivatives shown in Scheme 6.

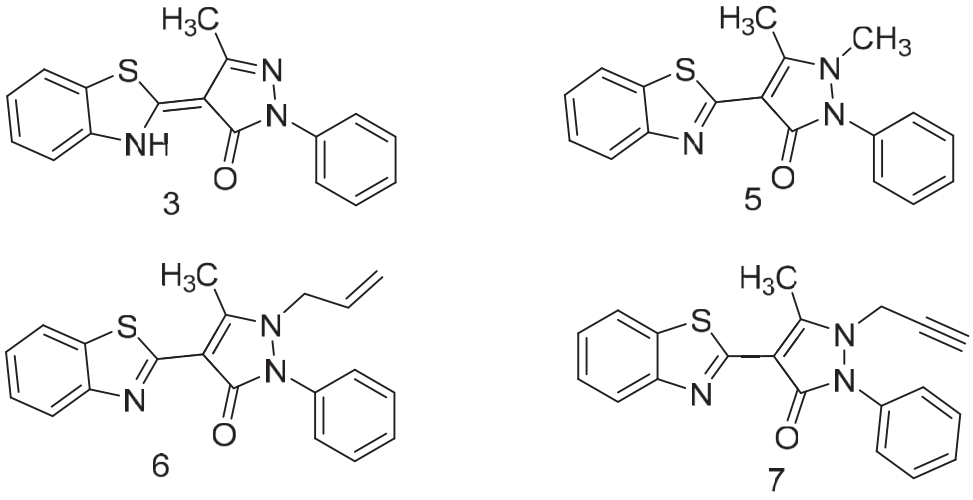

Scheme 6. Structures of compounds 3, 5, 6 and 7.

Table 4
Presentation of the percentage of cell viability compared to increasing concentrations (50−1.56 µg/ml) of the four compounds tested.

	Mit	3	5	6	7
50 µg/mL	3%	35%	70%	76%	116%
25 µg/mL	4%	53%	69%	85%	122%
12.5 µg/mL	9%	68%	87%	96%	146%
6.25 µg/mL	12%	74%	93%	123%	158%
3.12 µg/mL	40%	97%	99%	105%	175%
1.56 µg/mL	73%	142%	94%	134%	173%

intermolecular contacts are shorter (longer) than the van der Waals radii. The d_{norm} value is mapped onto the Hirshfeld surface by red, white or blue colors. The red regions represent closer contacts with a negative d_{norm} value while the blue regions represent longer contacts with a positive d_{norm} value. Moreover, the white regions represent contacts equal to the van der Waals separation and have a d_{norm} value of zero. As depicted in Fig. S1, the major interactions in the title compounds are the intramolecular H···O, H···N, and H···S hydrogen bonds.

The 2D fingerprint plots highlight particular atom pair contacts and enable the separation of contributions from different interaction types that overlap in the full fingerprint. Using the standard 0.6−2.6 views with the d_e and d_i distance scales displayed on the graph axes, the 2D fingerprint plot for **3** and **6'**are shown in Fig. S2. Including the reciprocal contactsfor **3,** the contribution of the H···O contact is the largest among the three hydrogen bonding interactions (Fig. S2). However, for **6′**, the largest contribution among the three hydrogen bonding interactions is the H···N contact (Fig. S2).

3.7. In vitro anticancer activity

The compounds containing pyrazole or benzothiazole moieties are heterocyclic compounds with interesting pharmacological activities. The study of their anti-tumor activity has grown considerably in recent years [36−44].

The first series of compounds combining a pyrazole and a thiazolidinedione nucleus was described in 2006 as having an inhibitory potential for CDC25 phosphatases which are involved in the multiplication of cells thus stopping the development of tumor cell lines [41]. Three other sets of molecules with similar structures have also been patented for three different types of activities:

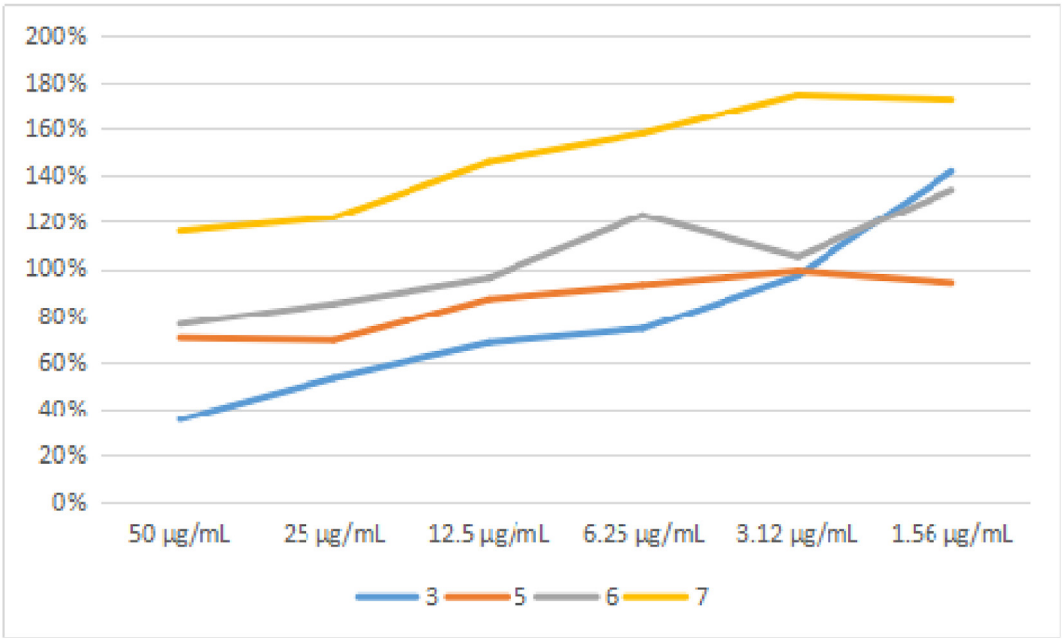

Fig. 8. Cytotoxic effects of 3, 5, 6 and 7 vis-a-vis the Hep2 line. The cells are incubated with increasing concentrations (50−1.56 µg/mL) for 48 h. Cell viability is assessed using the MTT test (n = 2). Mitomycin is used as a positive control of the test.

A first acts by blocking the ubiquitinylation and, therefore, the degradation of proteins involved in the cell cycle, thus causing the latter to stop [42].

A second has the effect of blocking the hypoxia signals that cause angiogenesis [43].

The third acts on the PIM kinases involved in cell proliferation [44] (Scheme 5).

The evaluation of the cytotoxicity of the products *in vitro* with respect to the Hep2 line was performed by measuring the cell viability using the MTT test. The cells were treated with the different synthetic products at increasing concentrations for 48 h (Table 4). Curves representing viability percentages as a function of the concentrations of the different products are presented in Fig. 8. The 50% inhibitory concentrations (IC_{50}) were calculated by extrapolation and the results are expressed as mean ± SD.

The curve for product **3** shows that there is a good dose-response correlation for the range of concentrations tested and the cytotoxic activity is proportional to the concentration of the products studied. The IC_{50}, the concentration at which we have 50% viability is on the order of 25 µg/mL. The Hep2 line remained unaffected by **5**, **6** and **7**. We did not observe a remarkable cytotoxic effect opposite the Hep2 line at the concentrations tested. The IC_{50} values for the different products are greater than 70 µg/mL for products **5** and **6.** For **7**, the IC_{50} value is greater than 100 µg/mL. It is worth taking note that **7** showed a cell viability larger than 100% no matter with its concentration. It could be ascribed to the fact that the MTT assay is a comparative method in general. The MTT assays give one some readout like the optical density, not the cell viability directly. If the optical densities of treated cells is 16% higher than that of the control group, the treated cells are not necessarily 16% more viable than the control group.

The study of the anti-tumor activity carried out on **3**, **5**, **6** and **7** proved to be interesting only for compound **3**. This applied at a concentration of the order of 28 µg/mL and was able to create cellular cytolysis of about 50%. On the other hand, **5** and **6** showed a medium cytotoxic activity while **7** has no effect on the tumor cells.

4. Conclusion

The use of the pyrazololylide-pyranopyrazolone rearrangement has been shown to be a new synthetic route for new heterocyclic systems containing benzothiazole and pyrazole moieties. Pyrazololylidepyrazolopyrone behaves like a heterocyclic 1,3-difunctional compound which undergoes nucleophilic attack-inducing opening reactions to give intermediates which cyclize later in different ways to lead to new compounds which are difficult to prepare by other synthetic routes. The alkylation reactions carried out on compound **3** allowed us to prepare a series of compounds from alkylation of nitrogen and carbon atoms at 4 and 2 positions of the pyrazolone moiety. It is worthy to note that the N-alkylated compound **5** has a similar structure to that of antipyrine in which the hydrogen atom at the 4-position of the pyrazole moiety was replaced by a benzothiazole nucleus.

The evaluation of the anticancer activities of these new compounds proved interesting only for 4-(1,3-benzothiazol-2-yl)-3-methyl-1-phenyl-2-pyrazolin-5-one (**3**). The alkylation of the pyrazole ring and the absence of a free NH group made these alkyl derivatives inactive.

Acknowledgements

The publication was prepared with the support of the "RUDN University Program 5−100". We thank Tulane University for support of the Tulane Crystallography Laboratory. We also thank the National Center for High-performance Computing (Taiwan) for providing computing time. Special thanks are also due to the reviewers and the editor for their helpful suggestions and comments.

Appendix A. Supplementary data

Supplementary data to this article can be found online at https://doi.org/10.1016/j.molstruc.2019.126910.

References

[1] P. Arora, V. Arora, H.S. Lamba, D. Wadhwa D, Importance of heterocyclic chemistry: a review, Int. J. Pharm. Res. Sci. 3 (2012) 2947–2955.
[2] W.-Q. Fan, A.R. Katritzky, in: A.R. Kartitzky, C.W. Rees, E.F.V. Scriven (Eds.), Comprehensive Heterocyclic Chemistry II, vol. 4, Elsevier Science, Oxford, UK, 1996, pp. 1–126.
[3] H.H. Wamhoff, in: A.R. Katritzky, C.W. Rees (Eds.), Comprehensive Heterocyclic Chemistry, vol. 5, Pergamon, Oxford, 1984, pp. 669–732.
[4] M. Maheshwari, A. Goyal, A review: synthesis and medicinal importance of 1,4-benzothiazine analogs, Asian J. Pharmaceut. Clin. Res. 8 (2015) 41–46.
[5] E.A. Sonawane, A.Y. Pawar, S.P. Nagle, P.P. Mahulikar, H. Dhananjay, Synthesis of 1,4-benzothiazine compounds containing isatin hydrazone moiety as antimicrobial agent, Chin. J. Chem. 27 (2009) 2049–2054.
[6] A. Napolitano, S. Memoli, G. Prota, A new insight in the biosynthesis of pheomelanins: characterization of a labile 1,4-benzothiazine intermediate, J. Org. Chem. 64 (1999) 3009–3011.
[7] N. Simon, D. Peles, K. Wakamatsu, S. Ito, Current challenges in understanding melanogenesis: bridging chemistry, biological control, morphology, and function, Pigm. Cell Melanoma Res. 22 (2009) 563–579.
[8] R.R. Gupta, P. Kumar, Synthesis of 6-trifluoromethyl-4h-1,4-benzothiazines as possible anticancer agents, J. Fluorine Chem. 31 (1986) 19–24.
[9] R.R. Gupta, R. Kumar, R.K. Gautam, Synthesis of 6-halogenated 4H-1,4-benzothiazines, J. Heterocycl. Chem. 21 (1984) 1713–1714.
[10] V. Srivastav, R. Gupta, R.R. Gupta, Single step synthesis of 4H-1,4-benzothiazines, Indian J. Chem. 39B (2000) 223–224.
[11] H. Sheibani, M.R. Islami, A. Hassanpour, K. Saidi, One-pot multi-component approach to the synthesis of 1,4-benzothiazines in aqueous media. PhosphorusSulfur Silicon Relat, Elements 183 (2008) 13–20.
[12] U.R. Pratap, D.V. Jawale, B.S. Londhe, R.A. Mane, Baker's yeast catalyzed synthesis of 1,4-benzothiazines, performed under ultrasonication, J. Mol. Catal. B Enzym. 68 (2011) 94–97.
[13] S.B. Munde, S.P. Bondge, V.E. Bhingolikar, R.A. Mane, A facile synthesis of 1,4-benzothiazines under solvent free conditions, Green Chem. 5 (2003) 278–279.
[14] S. Aloui, I. Forsal, M. Sfaira, M. Ebn Touhami, M. Taleb, M. Filali Baba, M. Daoudi, New mechanism synthesis of 1,4-benzothiazine and its inhibition performance on mild steel in hydrochloric acid, Port. Electrochim. Acta 27 (2009) 599–613.
[15] E.C. Alyea, A. Malek, Reaction products of 2-aminobenzenethiol with some β-diketones, J. Heterocycl. Chem. 22 (1985) 1325–1326.
[16] A. Dandia, P. Sarawgi, M.B. Hursthouse, A.L. Bingham, M.E. Light, J.E. Drake, R. Ratnani, Synthesis of a series of 2,3-disubstituted 4H-1,4-benzothiazines and X-ray crystal structure of ethyl 7-chloro-3-methyl-4H-1,4-benzothiazine-2-carboxylate, J. Chem. Res. 7 (2006) 445–448.
[17] Y. El Bakri, C.-H. Lai, J. Sebhaoui, A. Ben Ali, Y. Ramli, E.M. Essassi EM, J.T. Mague, Synthesis, crystal structure, Hirshfeld surface analysis, and DFT calculations of new 1-[(1-benzyl-1H-1,2,3-triazol-4-yl)methyl]-6-methoxy-1H-benzimidazol-2(3H)-one, Chem. Data Collect. 17–18 (2018) 472–482.
[18] A. Ben-Yahia, Y. El Bakri, C.-H. Lai, E.M. Essassi, J.T. Mague, Crystal structure, DFT calculations and Hirshfeldsurface analysis of 3-(4-methyl phenyl)-6-nitro-1H-indazole, Acta Crystallogr. E74 (2018) 1857–1861.
[19] I. Rayni, Y. El Bakri, C.-H. Lai, L. El Ghayati, E.M. Essassi, J.T. Mague, Synthesis, crystal structure, DFT calculations and Hirshfeld surface analysis of 2-(1-decyl-2-oxo-indolin-3-ylidene)propanedinitrile, ActaCryst E75 (2019) 21–25.
[20] Y. El Bakri, E.H. Anouar, I. Marmouzi, K. Sayah, Y. Ramli, M.E.A. Faouzi, E.M. Essassi, J.T. Mague, Potential antidiabetic activity and molecular docking studies of novel synthesized 3.6-dimethyl-5-oxo-pyrido[3,4-f][1,2,4]triazepino[2,3-a]benzimidazole and 10-amino-2-methyl-4-oxopyrimido[1,2-a]benzimidazole derivatives, J. Mol. Model. 24 (2018) 179.
[21] Y. El Bakri, E.H. Anouar, Y. Ramli, E.M. Essassi, J.T. Mague, Synthesis, crystal structure, spectroscopic characterization, Hirshfeld surface analysis, and DFT calculations of 1,4-dimethyl-2-oxo-pyrimido[1,2-a]benzimidazole hydrate, J. Mol. Struct. 1152C (2018) 154–162.
[22] B. Djerrari, E.M. Essassi, J. Fifani, B. Garrigues, M. Pierrot, Synthesis and crystal structure of 2-[1-phenyl-3-methyl-5-oxo-pyrazol-4-ylidene]-4-methyl-1,5-benzodiazepine, Indian J. Chem. B42 (2003) 2820–2827.
[23] C. Brown, R.M. Davidson, 1,4-Benzothiazines, dihydro-1,4-benzothiazines, and related Compounds, Adv. Heterocycl. Chem. 38 (1985) 135–176.
[24] Bruker, APEX3, SADABS, SAINT&SHELXTL, Madison, WI, 2016.
[25] G.M. Sheldrick, SHELXT. ActaCryst. A71 (2015) 3–8.
[26] G.M. Sheldrick, SHELXL-2014/7, ActaCryst C71 (2015) 3–8.
[27] A.D. Becke, Density-functional thermochemistry. III. The role of exact exchange, J. Chem. Phys. 98 (1993) 5648–5652.
[28] C. Lee, W. Yang, R.G. Parr, Development of the Colle-Salvetti correlation-energy formula into a functional of the electron density, Phys. Rev. B37 (1998) 785–789.
[29] A.C. Neto, E.P. Muniz, R. Centoducatte, F.E. Jorge, Gaussian basis sets for correlated wave functions. Hydrogen, helium, first- and second-row atoms, J. Mol. Struct. 718 (2005) 219–224.
[30] M.J. Frisch, G.W. Trucks, H.B. Schlegel, G.E. Scuseria, M.A. Robb, J.R. Cheeseman, G. Scalmani, V. Barone, G.A. Petersson, H. Nakatsuji, X. Li, M. Caricato, A.V. Marenich, J. Bloino, B.G. Janesko, R. Gomperts, B. Mennucci, H.P. Hratchian, J.V. Ortiz, A.F. Izmaylov, J.L. Sonnenberg, D. Williams-Young, F. Ding, F. Lipparini, F. Egidi, J. Goings, B. Peng, A. Petrone, T. Henderson, D. Ranasinghe, V.G. Zakrzewski, J. Gao, N. Rega, G. Zheng, W. Liang, M. Hada, M. Ehara, K. Toyota, R. Fukuda, J. Hasegawa, M. Ishida, T. Nakajima, Y. Honda, O. Kitao, H. Nakai, T. Vreven, K. Throssell, J.A. Montgomery Jr., J.E. Peralta, F. Ogliaro, M.J. Bearpark, J.J. Heyd, E.N. Brothers, K.N. Kudin, V.N. Staroverov, T.A. Keith, R. Kobayashi, J. Normand, K. Raghavachari, A.P. Rendell, J.C. Burant, S.S. Iyengar, J. Tomasi, M. Cossi, J.M. Millam, M. Klene, C. Adamo, R. Cammi, J.W. Ochterski, R.L. Martin, K. Morokuma, O. Farkas, J.B. Foresman, D.J. Fox, Gaussian 16, Revision A.03, Gaussian, Inc., Wallingford CT, 2016.
[31] M.A. Spackman, P.G. Byrom, A novel definition of a molecule in a crystal, Chem. Phys. Lett. 267 (1997) 215–220.
[32] J.J. McKinnon, M.A. Spackman, A.S. Mitchell, Novel tools for visualizing and exploring intermolecular interactions in molecular crystals, Acta Crystallogr. B60 (2004) 627–668.
[33] M.A. Spackman, D. Jayatilaka, Hirshfeld surface analysis, CrystEngComm 11 (2009) 19–32.
[34] M.J. Turner, J.J. McKinnon, S.K. Wolff, D.J. Grimwood, P.R. Spackman, D. Jayatilaka, M.A. Spackman, CrystalExplorer17, University of Western Australia, 2017. http://hirshfeldsurface.net.
[35] H.R. Kim, J. No, M.J. Seo, B.G. Song, B.S. Son, J.K. Kim, K.-R. Kim, H.G. Cheon, G.H. Lee, (5-(1,3-diaryl-1h-pyrazol-4-ylmethylene)-thiazolidine-2,4-dione Derivatives Useful as Anticancer Agent, Korea Research Institute of Chemical Technology, 2006. Patent WO2006/101307.
[36] R. Singh, U.V. Ramesh, D. Goff, G. Laidig, S.D. Issakani, J. Huang, D.G. Payan, J. Clough, Rhodanine Derivatives and Pharmaceutical Compositions Containing Them, Rigel Pharmaceuticals, Inc, 2004. Patent WO2004/043955.
[37] M. Cassin, G. Colella, S. De Munari, M. Grugni, Use of Thiazolidinone Derivatives as Antiangiogenic Agents, Cell Therapeutics Europe S.R.L., 2006. Patent WO2006/066846.
[38] S. Viveka, G. Vasantha, Dinesha, S. Naveen, N.K. Lokanath, G.K. Nagaraja, Synthesis, characterization, single crystal X-ray diffraction and DFT sktudies of ethyl 5-methyl-1-phenyl-1H-pyrazole-4-carboxylate, Mol. Cryst. Liq. Cryst. 629 (2016) 135–145.
[39] K. Karthik, A.D. Kumar, S. Naveen, K.A. Kumar, N.K. Lokanath, Synthesis, spectral characterization and X-ray crystal structure studies of 3-(benzo[d][1,3]dioxol-5-yl)-5-(3-methylthiophen-2-yl)-4,5-dihydro-1H-pyrazole-1-carboxamide: Hirshfeld surface, DFT and thermal analysis, J. Mol. Struct. 1161 (2018) 285–298.
[40] A.D. Kumar, S. Bharath, R.N. Dharmappa, S. Naveen, N.K. Lokanath, K.A. Kumar, Design, synthesis and spectroscopic and crystallographic characterisation of novel functionalized pyrazole derivatives: biological evaluation for their cytotoxic, angiogenic and antioxidant activities, Res. Chem. Intermed. 44 (2018) 5635–5652.
[41] L. Dakin, J. Dowling, M. Lamb, J. Read, Q. Su, X. Zheng, Chemical Compounds 251 Astrazeneca AB Patent WO2010/001169, 2010.
[42] B.K. Bhuyan, B.E. Loughman, T.J. Fraser, K.J. Day, Comparison of different methods of determining cell viability after exposure to cytotoxic compounds, Exp. Cell Res. 97 (1976) 275–280.
[43] J. Carmichael, W.G. DeGraff, A.F. Gazdar, J.D. Minna, J.B. Mitchell, Evaluation of a tetrazolium-based semiautomated colorimetric assay: assessment of chemosensitivity Testing, Cancer Res. 47 (1987) 936–942.
[44] T. Mosmann, Rapid colorimetric assay for cellular growth and survival: application to proliferation and cytotoxicity assays, J. Immunol. Methods 65 (1983) 55–63.